Overview of Physical Layer Enhancement for 5G Broadcast in Release 16

Dazhi He, Wanting Wang, Yin Xu, Xiuxuan Huang, Hao Cheng, Xiaohan Duan, Yihang Huang, Hanjiang Hong, Yiwei Zhang, and Wenjun Zhang, *Fellow, IEEE*

***Abstract*—3GPP is now carrying forward the development of the point to multipoint transmission mode of 5G on the basis of the cellular infrastructure and standard. Since the dedicated proposal for multimedia broadcast multicast system (MBMS) was approved, the MBMS technologies are evolving with the update of the requirements from 3G to 5G. This paper reviews the latest progress during the evolved MBMS standardization, which focuses on the LTE-based 5G terrestrial broadcast mode. Some agreements in terms of two widely discussed topics during 3GPP meetings, cell acquisition subframe (CAS) enhancement and numerology refinement, are presented. The enhancement of CAS and the update of numerology aim to deal with the service outage issue in the case of covering large area and serving high-mobility users. To verify the improvement brought by the CAS enhancement and the new numerology, simulations from system level and link level are carried out by several organizations and the representative results are presented and analyzed in this paper.**

***Index Terms*—LTE-based 5G terrestrial broadcast, new numerology, CAS enhancement, system level simulation, link level simulation.**

I. Introduction

DIGITAL television broadcast networks employ the same radio resources to provide the same content to a wide range of users, which enables higher resource utilization compared with the traditional unicast delivery network. Multimedia Broadcast/ Multicast System (MBMS), proposed by the 3rd Generation Partnership Project (3GPP) standardization organization, incorporates the multicast/ broadcast services into a cellular network [1].

In 2004, 3GPP approved 3G-based MBMS technology for the first time in Release 6 (Rel-6) [2]. A service of MBMS was defined to cover the terminal, radio network, core network and user service aspects. The MBMS not only allows the delivery of low-rate message-like data, but also supports the multicast and broadcast of high-speed multimedia services.

Manuscript received December 2, 2019; revised February 27, 2020; accepted March 3, 2020. Date of publication April 8, 2020; date of current version June 5, 2020. This was supported in part by the National Natural Science Foundation of China under Grant 61671297, in part by the Shanghai Natural Science Foundation under Grant 19ZR1426600, in part by the Shanghai Key Laboratory of Digital Media Processing under Grant STCSM 18DZ2270700, and in part by the Startup Fund for Youngman Research at SJTU (SFYR at SJTU). *(Corresponding author: Yin Xu.)*

The authors are with Cooperative Medianet Innovation Center, Shanghai Jiao Tong University, Shanghai 200240, China (e-mail: xuyin@sjtu.edu.cn).

Color versions of one or more of the figures in this article are available online at http://ieeexplore.ieee.org.

Digital Object Identifier 10.1109/TBC.2020.2981775

With the advancement of the Long Term Evolution (LTE) standard, in 2009, 3GPP approved to study evolved MBMS (eMBMS) in Rel-9 [3] to improve the transmission performance of MBMS. Based on more intensive research, in the subsequent versions of Release 10 (Rel-10) [4], Release 11 (Rel-11) [5], and Release 12 (Rel-12) [6], 3GPP brought in extra key functionalities, such as counting and admission control to support a wider coverage of Multicast/Broadcast Single Frequency Network (MBSFN). In Release 14 (Rel-14), 3GPP introduced eMBMS-enhancement [7], which is also referred as LTE-based Enhanced Television (EnTV). EnTV provides a Receive-Only Mode that each user equipment (UE) does not rely on the sim card to access the network. It supports the transmission of high-definition and ultra-high-definition videos. In 2017, eMBMS-enhancement was frozen during Rel-14 [8]. Reference [9] reviews the evolution of physical layer in MBMS since Rel-9.

As the development of 5G standard, it was found that some requirements for the 5G radio access technology (RAT) in [10] could not be fulfilled by eMBMS-enhancement in Rel-14. Therefore, at the 3GPP RAN #80 meeting held in San Diego [11], a study item (SI) of LTE-based 5G terrestrial broadcast was launched for the ongoing 5G study of Release 16 (Rel-16) [12]. The transmission capability of the LTE-based EnTV was studied in this research project and the gap between the transmission capability and expected requirements of broadcast service was analyzed. Meanwhile, some solutions were provided to narrow this gap and to finally achieve 5G enhancement. During the SI stage, it is identified that the gap mainly lay in the Req.7 and Req.8 in [13].

Req.7 is to support service over large geographic area of an entire country and/or cell size of 100 km in the fixed reception (rooftop) scenarios. Req.8 requires the network to support stable reception under different mobility scenarios, which include scenarios with fixed, portable and mobile UEs and vehicles with speeds up to 250km/h. To meet these two requirements, during SI stage, different companies/universities have proposed various solutions, such as multicast synchronous transfer (MUST) from Huawei, cell acquisition subframe (CAS) from EBU and non-uniform constellation (NUC) from Shanghai Jiao Tong University [13]. After discussion and analysis, it is widely recognized that two different numerologies shoud be defined in work item to meet these two requirements separately. On the other hand, 5G-Xcast project targeting at the 5G broadcast and multicast enabler is in progress and a lot of researches have

been conducted to provide some alternative New Radio (NR) options for 5 G terrestrial broadcast services [7], [14], [15]. Coding and modulation enhancements for 5G terrestrial broadcast are also proposed and analyzed in [16]. This paper focuses on two widely discussed topics in 3 GPP, the new numerology and enhancement of CAS in LTE-based 5G terrestrial broadcast. Extensive simulations are carried out from both system and link aspects to verify the improvement and some agreements reached during work item stage were concluded.

The rest of this paper is structured as follows. The frame structures and CAS of eMBMS-enhancement in Rel-14 are introduced in Section II respectively. Section III presents the study of new numerologies and some enhancement schemes of CAS to fulfill the requirement of 5G RAT. In Section IV, the performances of different new numerologies obtained from system-level simulations (SLSs) and link-level simulations (LLSs) are presented. Besides, performances of different CAS enhancement schemes are also compared in this section. Finally, the conclusion is drawn in Section V.

II. Frame Structures and CAS in eMBMS-Enhancement

New numerologies and CAS enhancement schemes are studied for the LTE-based terrestrial broadcast during the work item (WI) stage. Thus, in this section, frame structures and CAS structure of eMBMS-enhancement in Rel-14 are briefly introduced.

A. Frame Structure of eMBMS-Enhancement

In Rel-7, 3GPP defined a new MBMS transmission mode based on single frequency network, MBSFN, which enables synchronous transmission by multiple cells using the same frequency. The introduction of MBSFN solves the interference problem of MBMS at the boundary of the community and improves the overall throughput. In the subsequent version, 3GPP proposed eMBMS technology and extend the length of cyclic prefix to support larger MBMS coverage. However, due to the technical limitations, only 60% of the subframes can be allocated to MBMS service and high bit rate transmission is not supported.

In order to further improve the transmission performance of the MBMS system, 3GPP approved the eMBMS-enhancement in Release14 in 2017. The length of the SFN cyclic prefix (CP) was further extended to 200μs to support a wider range of SFN. In addition, to obtain higher capacity for broadcast service, CAS with an increased interval was employed in Release 14 to reduce synchronization overhead. In addition, the new subframe was designed with almost 100% eMBMS carrier allocation without unicast control region. The schematic diagram of the transmission mode with 100% MBSFN service is shown in Fig. 1.

The LTE frame has a duration of 10 ms and consists of 10 subframes where each subframe has a duration of 1 ms. The subframe is composed of N_{sb} Orthogonal Frequency Division Multiplexing (OFDM) symbols, each having a total duration of $T_s = T_u + T_{CP}$ where T_u is the symbol duration and T_{CP} is the duration of CP. In all cases, the percentage of the overhead

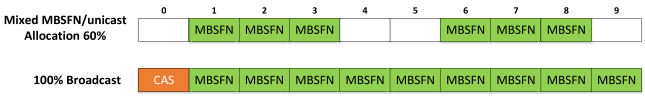

Fig. 1. 60% allocation of mixed MBSFN/unicast and 100% broadcast in Rel-14.

TABLE I
Numerologies in Release 14

CP mode	Δf (kHz)	OFDM symbols per subframe	Subcarriers per Resource Block	T_{cp} (μs)	T_u (μs)	ISD
Extended	15	12	12	16.7	66.7	5
	7.5	6	24	33.3	133.3	10
	1.25	1	144	200	800	60

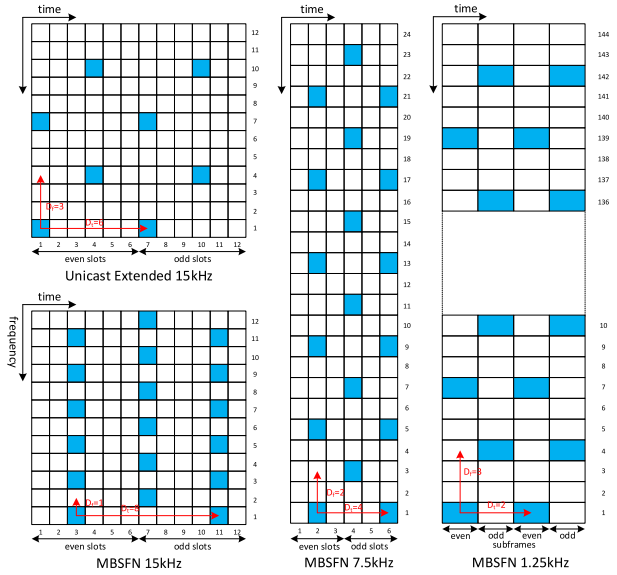

Fig. 2. Reference signals of MBSFN and unicast subframes in Rel-14.

due to the CP is 20%. Physical Resource Block (PRB) is a basic allocating unit occupying 180 kHz bandwidth. Each PRB is constituted by N_{sc} Resource Elements (REs), which have a subcarrier spacing of Δf. Different values of Δf and related frame structure parameters for MBSFN subframes are defined in Rel-14, which are summarized in TABLE I. As shown in TABLE I, the maximum supported inter site distances (ISDs) for the two short CPs are 5 km and 10 km, which are only applicable in low-power-low-tower (LPLT) scenario. The use of new CP extends the ISD up to 60 km which can be used in high-power-high-tower (HPHT) deployments.

The selection of particular OFDM parameters has an impact on the structure of the frames. Compared with the unicast mode, the eMBMS modes have an associated set of reference signal patterns. Each cell belonging to the MBSFN region transmits the same MBSFN reference signal with exactly the same time-frequency resources. Fig. 2 shows the reference signal patterns of MBSFN subframes and unicast subframes given different numerologies [14].

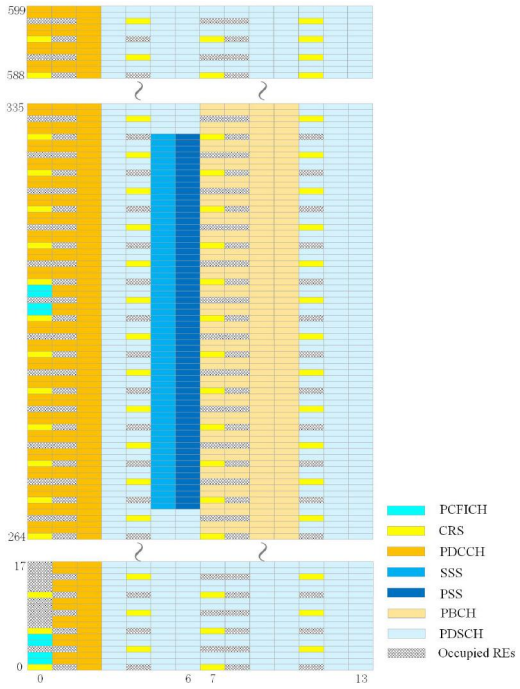

Fig. 3. Structure of CAS with Bandwidth 10MHz, Cell ID 0, CFI 3 and normal CP.

B. CAS Structure of eMBMS-Enhancement

Cell acquisition subframe (CAS) is a new type of subframe used for synchronization and basic signaling transmission in the eMBMS-enhanced dedicated transmission mode. CAS inherits the traditional parameters of the LTE system, that is, a subcarrier spacing of 15 kHz and a cyclic prefix length of 4.7μs (normal) or 16.7μs (extended). CAS is located in the 0^{th} subframe and its transmission time interval is 40ms. CAS includes the broadcast synchronization signal (PSS and SSS) and basic system information, such as master information block (MIB) carried by PBCH, downlink control information carried by PDCCH and a part of system information block (SIB1 and SIB13) carried by PDSCH. The structure of CAS is shown in Fig. 3 (Each grid represents a resource element (RE) and the figure only shows the mapping relation under certain parameters.)

PSS and SSS (Primary and Secondary Synchronization Signals): In the frequency domain, PSS and SSS are mapped to the central 62 sub-carriers regardless of the system bandwidth, and in the time domain, PSS is transmitted in the last symbol of slot 0 of CAS, while SSS is sent one symbol earlier [17]. When the PSS and SSS are detected by UE, the physical cell identity can be decoded. Meanwhile, by identifying the positions of PSS and SSS, the receiver is able to find the start of a 10 ms frame, which helps to achieve the downlink synchronization.

PBCH (Physical Broadcast Channel): In the frequency domain, PBCH is mapped to the central 72 sub-carriers regardless of the system bandwidth, and in the time domain, it is situated in the first four OFDM symbols of slot 1 [17]. The MIB carried by PBCH includes: downlink bandwidth, the upper 8 bits of the 10-bits System Frame Number (SFN), and PHICH configuration information, which mainly indicates the REs reserved for the physical hybrid ARQ indicator channel (PHICH).

PDCCH (Physical Downlink Control Channel): CAS starts with control channels such as physical control format indicator channel (PCFICH), PHICH and PDCCH. PHICH carries the hybrid-ARQ ACK/NACK (Automatic Repeat-reQuest Acknowlegement/Negative Acknowledgement). However, the information carried by PHICH is not used in MBMS-dedicated cells and hence the corresponding REs are empty. PCFICH, occupying 16 REs of the first OFDM symbol, carries control format indicator (CFI), which indicates the number of OFDM symbols used for transmission of PDCCHs in a CAS. PDCCH carries DCI (Downlink Control Information), which includes scheduling assignments and other control information for one or more UEs [18]. In general, there may be multiple PDCCHs within one subframe. The UE needs to first demodulate DCI in PDCCH before demodulating PDSCH at the corresponding resource location.

PDSCH (Physical Downlink Shared Channel): In the time domain, PDSCH fills all OFDM symbols (excluding REs that are occupied), and in the frequency domain, the position is determined by the content of DCI. The system information includes master information block and multiple system information blocks, wherein the PDSCH is used to transmit SIB 1 and SIB 13. SIB 1 is used to define the scheduling way of other SIBs, and includes the parameters of cell selection; SIB 13 contains MBMS control information associated with one or more MBSFN areas [18].

III. Enhancements in Rel-16

Frame structure and CAS structure in Release 14 cannot fulfill the requirement of 5G RAT, especially for the requirement of covering large geographic area and serving high-mobility users. Thus, during the WI of LTE-based 5G terrestrial broadcast, new numerologies (frame structures) and CAS enhancements are mainly studied. In this section, the progress of new numerologies and some enhancement candidates of CAS are introduced.

A. New Numerologies

In this section, the design of new OFDM frame structures for the new numerology is presented in addition to the existing ones with CPs of 16.67μs, 33.33μs and 200μs. Furthermore, the possible designs of reference signal (RS) pattern are proposed for the new numerology.

Since a longer CP length can provide wider coverage and a larger sub-carrier spacing can provide stronger robustness in high mobility scenarios, Rel-16 introduces two new CP length of 100μs and 300μs for car-mounted and rooftop reception respectively [19]. The newly investigated CP length of 100μs can be used to support transmission with a maximum speed of 250km/h in car-mounted reception of LPLT scenario. Numerology with CP duration of 300μs is adopted by middle power middle tower (MPMT) and HPHT scenarios to support 100 km coverage for rooftop reception. TABLE II summarizes the frame structures with respect to the new numerologies.

TABLE II
NUMEROLOGIES IN RELEASE 16

Δf (kHz)	OFDM symbos per subframe	Subcarrier per Resource Block	T_{cp} (μs)	T_u (μs)	ISD(km)
2.5	2	72	100	400	30
0.37	1	486	300	2700	100

TABLE III
APPLICATION SCENARIOS

Scene	Configuration	ISD(Inter site distance)
1	MPMT	~50km
2	HPHT-1	~125km
3	HPHT-2	~173km
4	LPLT	~15km

The ISD supported by different transmission scenarios are summarized in the following TABLE III. Among the four scenarios, scenario 4 is the most common LTE transmission scenario. The expected ISDs for rooftop and car-mounted receptions in Rel-16 were significantly extended in all scenarios. The corresponding frame structure and the size of the transport block will be further discussed in terms of the new numerology.

The frame structure related to the numerology with a CP length of 300μs and OFDM symbol duration of 2700μs is presented. Due to the increase of CP length, the duration of the legacy subframe is now extended to 3ms and only one OFDM symbol is included in each subframe. The frequency resource occupied by each resource block remains unchanged, and the number of subcarriers in each resource block is now 486. For MBMS-dedicated carrier, the CAS is transmitted every 40ms and the MBSFN subframes occupy the remaining 39ms. Therefore, the CAS precedes 13 MBSFN subframes.

For the design of RS pattern, two parameters need to be determined: 1) D_f is the space between the subcarriers carrying RS in the frequency domain. Note that the RS subcarriers are not necessarily located in the same OFDM symbol and 2) D_t, which is the difference in OFDM symbol number between successive RSs on a given subcarrier in time domain.

In LTE system, in order to guarantee the performance of channel estimation, Nyquist sampling theorem needs to be met. According to the two-dimensional Nyquist sampling theorem, the interval of RSs in frequency and time domain of LTE system is:

$$D_f \leq (4\tau_{max}\Delta f)^{-1}, \quad D_t \leq (4f_d T_s)^{-1}$$

where f_d is the Doppler frequency shift, τ_{max} is the multipath delay, Δf is sub-carrier spacing and T_s is the symbol duration.

Given the analysis above, some combination candidates of D_f and D_t are evaluated. Fig. 4 gives one example of RS patterns with $D_f = 2$ and $D_t = 2$. System and link level simulations are performed to determine the appropriate RS patterns.

Transport block size (TBS) determines the number of bits of the transport block in one subframe. For a given bandwidth and Modulation and Coding Scheme (MCS), a corresponding

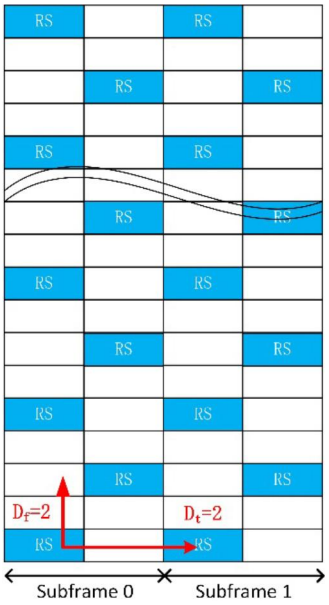

Fig. 4. Scattered pattern with $D_f = 2$, $D_t = 2$.

TBS can be obtained by looking up the TBS table. However, for the new numerologies with subcarrier spacing of 0.37 kHz to support rooftop reception, the symbol duration is longer than 1ms which exceeds the length of one legacy subframe. If the TBS tables in 3GPP TS 36.213 are re-used, the TBS determined by the original table is significantly smaller than the actual number of bits that can be transported. There is one possible method to modify the TBS table, which can be used for the new numerology. The specific modification steps are as follows.

S1: Reuse the transport block size table in TS 36.213 and obtain the corresponding TBS according to the I_{TBS} in [20].

S2: Calculate the used TBS' as $TBS' = \text{round}\{TBS \times \alpha\}$, where the round operation maps $TBS \times \alpha$ to the closest TBS in the legacy TBS tables.

In the case of two TBSs having the same distance of $TBS \times \alpha$, the larger TBS is chosen. The value of α is fixed as $\alpha = 3$ in the specification.

B. CAS Enhancements

According to the requirements of 5G radio access, the new RAT (Radio Access Technology) should specifically allow for multicast/broadcast services occupying up to 100% of downlink resources (100% means a dedicated MBMS carrier). Therefore, based on the original CAS structure, some adjustments need to be made to improve the performance of reception. We mainly focus on enhancements of the PBCH and PDCCH structure.

1) PBCH Enhancement: The performance of PBCH is indicated by the SNR requirements given a BLER constraint. To reduce the SNR requirement, one widely adopted method is to transmit the PBCH repeatedly. The reserved resources for the repeated PBCH are shown in Fig. 5. (Each grid represents a Resource Block in the frequency domain and PDCCH

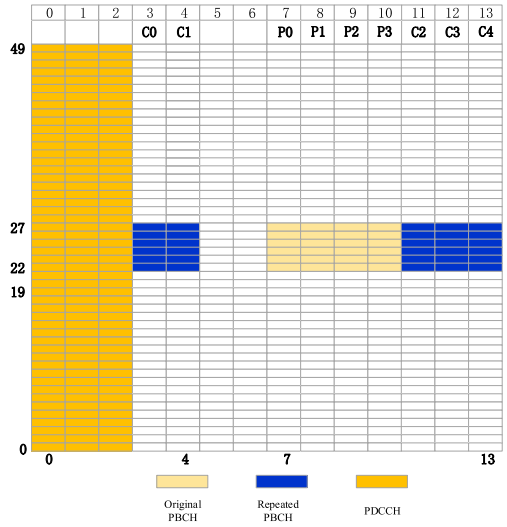

Fig. 5. Resource Reservation for the Repeated PBCH.

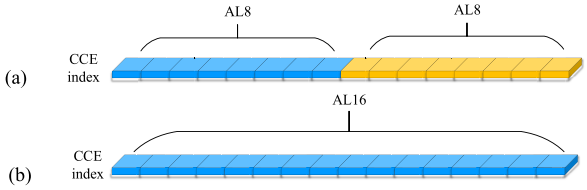

Fig. 6. Different Aggregation Level.

occupies 3 OFDM symbols according to the CFI value in Fig. 3.)

The repeated PBCH is mapped to the same position as the original PBCH in frequency domain but occupies different OFDM symbols in the time domain, whose indices are respectively C0-C4 as shown in Fig. 5. We denote the indices of the original PBCH symbols as P0-P3. In the time domain, the PBCH occupies only 4 OFDM symbols, and the repetitive PBCH occupies another 5 OFDM symbols. In order to fill up the central 72 sub-carriers in the frequency domain, some PBCH symbols need to be repeated twice. It can be seen from the structure of CAS in Fig. 3 that P0 and P1 can only be copied to symbols {C1,C2} in the CAS due to the existence of CRS, and P2 and P3 can be copied to symbols {C0, C3, C4}. Based on the considerations above, there are twelve candidate repetition schemes as shown in TABLE IV [21]. However, it has not been decided yet which specific mapping method of the repetitive PBCH in the table is used.

2) PDCCH Enhancement: The reception performance of PDCCH is closely related to its Aggregation Level (AL). The AL indicates how many control channel elements (CCEs) are used to transmit PDCCH, where CCE is the basic unit for PDCCH transmission. Four aggregation levels of 1, 2, 4 and 8 have been specified. The larger the AL, the more resources are occupied by the PDCCH. At the receiver side, the reception performance improves along with the increase of the AL. Based on these analyses, two possible methods are proposed.

Method 1: Repeat PDCCH and transmit both the original and the repeated PDCCH as shown in Fig. 6(a) [22].

TABLE IV
MAPPINGS OF ADDITIONAL PBCH SYMBOLS TO EMPTY OFDM SYMBOLS WITHIN A CAS

Scheme Number	Copies of PBCH symbols appearing in the ordered symbol indices {C0,C1,C2,C3,C4} within a CAS subframe
0	$\{P_2, P_0, P_1, P_2, P_3\}$
1	$\{P_2, P_0, P_1, P_3, P_2\}$
2	$\{P_3, P_0, P_1, P_2, P_2\}$
3	$\{P_3, P_0, P_1, P_3, P_2\}$
4	$\{P_3, P_0, P_1, P_2, P_3\}$
5	$\{P_2, P_0, P_1, P_3, P_3\}$
6	$\{P_2, P_1, P_0, P_2, P_3\}$
7	$\{P_2, P_1, P_0, P_3, P_2\}$
8	$\{P_3, P_1, P_0, P_2, P_2\}$
9	$\{P_3, P_1, P_0, P_3, P_2\}$
10	$\{P_3, P_1, P_0, P_2, P_3\}$
11	$\{P_2, P_1, P_0, P_3, P_3\}$

Method 2: Increase the resources reserved for PDCCH, that is, increase the maximum available AL by resorting to some techniques, such as rate matching, and specify AL16 [23].

IV. PERFORMANCE EVALUATION

In this section, system-level simulations (SLSs) and link-level simulations (LLSs) are conducted to evaluate the performance of different new numerologies and different RS patterns correspondingly. Performance of different CAS enhancement schemes are also compared in this section.

A. Simulation Platform

As shown in Fig. 7, system-level simulation and link-level simulation are performed by building a simulation platform to determine and evaluate new numerologies for different scenarios supporting the 5G RAT requirements. After the new numerologies are approved in 3GPP meetings, system-level simulation is used to obtain a SINR threshold for link level simulation. This threshold determines the TBS and MCS that the link-level simulation used to evaluate the performances of different schemes of new numerologies.

Based on the Vienna platform [24], we introduce some new features into this platform to achieve LTE-based 5G terrestrial broadcast transmission. New subcarrier spacing parameters for LTE-based 5G terrestrial broadcast, antenna model and large-scale fading of ITU are introduced in the simulator. The process of SLS consists of the following steps:

- Generate network topology
- Generate UE distributions
- Generate channel coefficients
- Calculate the SINR of each UE
- Calculate the CDF of the SINR

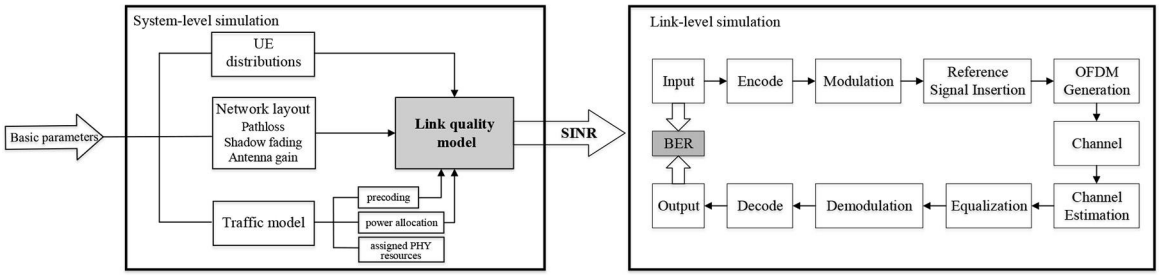

Fig. 7. Simulation platform.

TABLE V
PARAMETERS FOR LINK-LEVEL SIMULATION

Parameter	Value
System bandwidth	10 MHz
Carrier frequency	700 MHz
Sub-carrier spacing	2.5kHz/0.37kHz
Channel model	TDL-B
Delay Spread	LPLT:20μs; MPMT:35μs; HPHT-1:45μs
Number of TX antennas at the UE	Rooftop:1; Car-mounted:2
Number of RX antennas at the UE	2
Channel Estimation at Rx	One-dimensional linear interpolation in time and frequency domain
Turbo Decoding Algorithm	Max-Log-MAP with a maximum of 8 iterations

After the SINR threshold is given by SLS, TBS and MCS for LLS can be determined from the TS 36.211. The process of LLS consists of the following steps:

- Encode and modulation
- Reference signal insertion and OFDM generation
- Channel estimation and equalization
- Demodulation and decode
- Calculate the bit error rate (BER).

B. Simulation Results of New Numerology

From SLS results of LTE-based 5G terrestrial broadcast presented in [25], [26], [27], it can be observed that longer CP is able to extend ISD for the HPHT/MPMT rooftop reception and the numerology of Tcp = 300μs/Tu = 2.7 ms has the highest spectral efficiency in most cases. Thus, it is specified in 3GPP meetings. In addition, the new numerology of Tcp = 100μs/Tu = 400μs is a good compromise considering the Doppler resistance and coverage requirement for the LPLT car mounted reception.

The main simulation assumptions are detailed in TR 36.776. A summary of the most relevant parameters of this paper is detailed in TABLE V.

The channel model selected in LLS is the TDL-B with a Delay Spread (DS) of 20μs, 35μs and 45μs for LPLT, MPMT and HPHT-1 respectively, which is obtained according to SLS in [27]. Regarding the channel estimation algorithm at the receiver, the UE performs independent one-dimensional linear interpolation in time and frequency domains, which is recommended by [25].

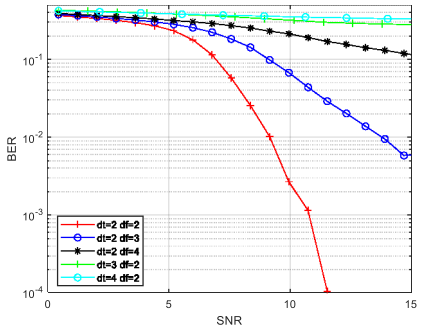

Fig. 8. BER performance of different combination of D_t and D_f at the speed of 250km/h.

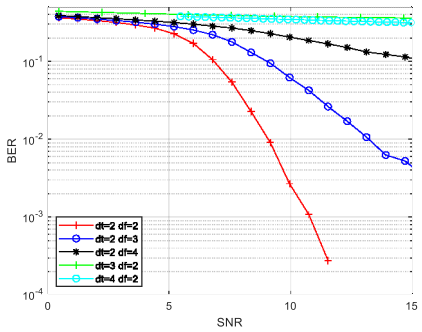

Fig. 9. BER performance of different combination of D_t and D_f at the speed of 150km/h.

The simulation results and analyses of RS patterns for LPLT car-mounted reception and HPHT/MPMT rooftop reception are presented respectively in the following.

1) Car-Mounted Reception: As mentioned in Section II, the specific value of D_f and D_t should be considered in the design of RS pattern. RS overhead and system performance are two important factors for the selection of D_f and D_t. The larger D_f is, the smaller RS overhead and equalization interval (EI) are. Therefore, there is a trade-off to find the appropriate combination of D_t and D_f.

Fig. 8 and Fig. 9 compare the BER performance of different combinations of D_t and D_f at the speed of 250 km/h and 150 km/h [28]. Here D_f is used to represent the RS tone separation in the frequency domain and D_t is used to represent the RS tone separation in the time domain. From LLS results, it can be seen that the RS pattern with $D_f = 2$ and $D_t = 2$ can provide the best BER performance.

TABLE VI
SPECTRAL EFFICIENCIES FOR LPLT SCENARIOS

D_f	D_t	RS overhead	95%-tile SINR (dB)	SE @ 150km/h (bps/Hz)	SE @ 250km/h (bps/Hz)
2	2	25%	9.0	1.11	0.97
2	4	12.5%	9.0	0.97	0.78
3	2	16.7%	7.6	0.96	0.85
3	4	8.3%	7.6	0.85	0.68
4	2	12.5%	6.9	0.85	0.85
4	4	6.25%	6.9	0.78	0.68

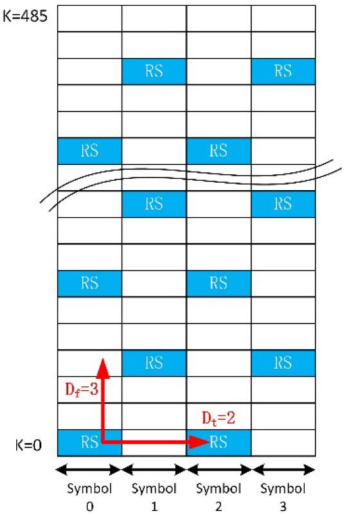

Fig. 10. Rhombic RS pattern with $D_f = 3$ and $D_t = 2$.

TABLE VI gives the 95%-tile SINR thresholds and spectral efficiencies in terms of different RS patterns in LPLT scenario. As shown in Table VI, with this threshold as a reference, the real-time throughputs of the system are evaluated and the spectral efficiency are calculated. It can be seen that $D_f = 2$ has a larger spectral efficiency compared with $D_f = 3$. The reason is that the SINR gain of longer EI is higher than the SINR loss of larger RS overhead. Comparing the spectral efficiency values of different RS patterns with Tcp ='100μs/Tu = 400μs, the RS pattern of $D_f = 2$ and $D_t = 2$ has the maximum spectral efficiency value among all the 6 cases. Thus, the RS pattern of $D_f = 2$ and $D_t = 2$ is specified for the new numerology of Tcp = 100μs/Tu = 400μs to support mobility of up to 250km/h in Rel-16.

2) Rooftop Reception: For MPMT and HPHT-1 scenarios, staggered RS pattern proposed by Qualcomm [29] and rhombic RS patterns proposed by Huawei [26] and Shanghai Jiao Tong University [30] to support larger coverage in rooftop reception are introduced and analyzed in this section. Fig. 11 depicts the staggered RS pattern with $D_f = 3$ and $D_t = 4$, where the RSs from 4 consecutive symbols are coalesced together. Fig. 10 shows the rhombic RS pattern with $D_f = 3$ and $D_t = 2$ [30].

TABLE VII summarizes the 95%-tile SINR thresholds and the spectral efficiency values for rooftop reception with the rhombic RS pattern and the staggered RS pattern, respectively. It can be seen from TABLE VII, for both HPHT-1 and

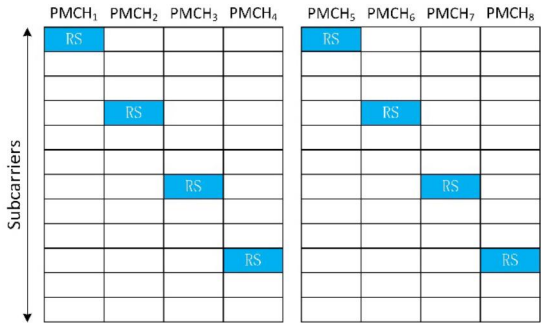

Fig. 11. Staggered RS pattern with $D_f = 3$ and $D_t = 4$.

TABLE VII
95%-TILE SINR AND SPECTRAL EFFICIENCY VALUES OF THE MIXED CARRIER FOR ROOFTOP RECEPTION

Network Topology	Pattern	Df	Dt	95%-tile SINR (dB)	Spectral efficiency (bps/Hz)
HPHT-1	Rhombic	3	2	10.9	1.65
HPHT-1	Staggered	3	4	9.4	1.52
MPMT	Rhombic	3	2	18.4	2.75
MPMT	Staggered	3	4	14.9	2.47

TABLE VIII
CAS SNR THRESHOLD IN A FADING CHANNEL

Scenario	95% SNR/dB	99% SNR/dB
LPLT	-3.2	-5.9
MPMT	-1.2	-3.7

TABLE IX
LINK LEVEL SIMULATION OF PBCH AND PDCCH IN LPLT NETWORK WITH BLER = 0.01

	SNR requirement/dB	
	Fd = 2Hz(3km/h)	Fd = 163Hz(250km/h)
PBCH	2.4	2.5
PDCCH (AL=8)	-3.6	-3.8

MPMT rooftop scenarios, the rhombic RS pattern with $D_t = 2$ performs better in terms of spectral efficiency.

The simulation results in [31] show that the performance of the staggered RS pattern with $D_t = 4$ is better than that with $D_t = 1/2/3$ when TBS is as large as 71112 bits. When TBS is set as a small value of 45352, the performance difference for the staggered RS pattern with different D_t value is small.

Therefore, both the staggered RS pattern with $D_f = 3$ and $D_t = 4$ and rhombic RS pattern with $D_f = 3$ and $D_t = 2$ are supported in the case of rooftop reception given Tcp = 100μs/Tu = 400μs.

C. Link-Level Simulation Results for CAS

Reference [23] and [32] analyzed the gap between the reception performance of CAS in the car-mounted scenario and the new requirements of LTE-based 5G terrestrial broadcast through system-level and link-level simulation. The results of SNR threshold and requirements are shown in TABLE VIII and IX.

TABLE X
SIMULATION PARAMETERS OF CAS

Doppler Shift	Bandwidth	Delay Spread	Cyclic Prefix	Channel Model
163Hz	10MHz	2μs	4.7μs	TDL-B

TABLE XI
LINK LEVEL SIMULATION RESULTS OF REQUIRED SNR FOR 1% BLER FOR PDCCH WITH DIFFERENT AL

	AL8	AL16	AL8+AL8
SNR/dB	-5.2	-7.3	-7.2

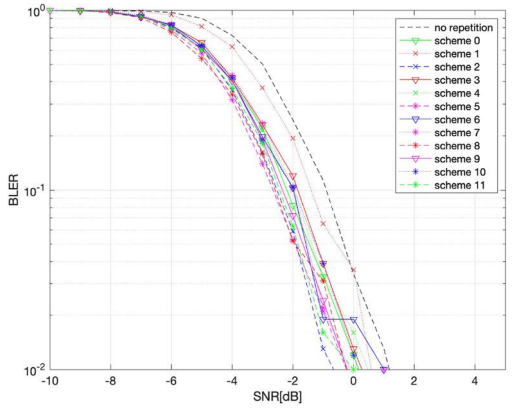

Fig. 12. Link level evaluation of different mappings of additional PBCH symbols.

According to the system-level evaluation (TABLE VIII), the SNR with 99% coverage probability is −5.9 dB (LPLT) and −3.7dB (MPMT) in the car-mounted scenario, which indicates that LPLT is the more challenging scenario in terms of SNR requirements. According to the link level evaluation (TABLE IX), the SNR requirements for correctly decoding the PBCH and PDCCH are 2.4dB and −3.8dB, respectively, which means the 99% percentile SNR obviously cannot meet the expected SNR requirement. Therefore, several methods are proposed to improve PBCH reception performance as introduced in Section III. Simulations are performed with the parameters summarized in TABLE X.

1) Link Level Evaluation of PBCH: Link-level evaluation results of different mappings for PBCH reception mentioned in Table IV is shown in Fig. 12.

Obviously, the use of PBCH repetition reduces the SNR requirement of PBCH reception. A proper mapping can provide significant SNR gain and up to 2dB gain can be observed by the Scheme 2 proposed by Qualcomm. Therefore, the OFDM symbol indices C0-C4 is specified for the repeated PBCH. However, difference of the SNR gains caused by different mapping schemes is small, so it has not been determined which one in TABLE IV to be used in [33].

2) Link Level Evaluation of PDCCH: Based on the link level parameters of [22], the two enhancement methods of PDCCH mentioned in Section III-B are simulated. Results are shown in TABLE XI.

When the aggregation level is 8, the SNR requirement of PDCCH reception is −5.2 dB. When the method of PDCCH repetition with AL8 (Method 1, as shown in Fig. 6(a)) is used, the SNR requirement is −7.2 dB and the SNR gain is 2 dB; if the AL16 method (Method 2, as shown in Fig. 6(b)) is used, the SNR requirement is −7.3 dB and the SNR gain is 2.1 dB. In terms of performance gain, the difference between the two methods is small.

For Method 1, there is no difficulty for the legacy UE to decode the original PDCCH, but the decoding of the repeated PDCCH may be infeasible. If the DCI is scrambled with a different scrambling sequence from the original PDCCH, the obtained PDCCH cannot be recognized by the legacy UE; if the same scrambling sequence is used to scramble the DCI, according to the restrictions mentioned in TS 36.302 [34], a UE may ignore the additional DCI. Therefore, this method may not achieve the desired effect. In summary, the behavior of the legacy UE upon receiving two identical PDCCHs with AL8 is unpredictable. For Method 2, it considers the problem of backward compatibility, and there is no unpredictability compared to Method 1, but the use of this method requires specification of new aggregation level, i.e., AL16.

Therefore, considering the backward compatibility and the consistency of legacy UE's behavior, Method 2 proposed by Qualcomm, i.e., AL16, is specified for PDCCH enhancement.

V. CONCLUSION

This paper reviews the latest progress with respect to the ongoing study of LTE-based terrestrial broadcast in 3GPP standardization meetings. Some enhancement schemes of CAS and two new numerologies specified in LTE-based terrestrial broadcast of Release 16 are presented. CAS enhancement is used to guarantee the more robust reception of the control signaling carried by the PBCH and PDCCH. The introduction of two new numerologies aims to support rooftop reception with 100km coverage and mobile reception with mobility up to 250km/h respectively. Theoretical analysis and simulation results in this paper provide an insight about the technical details specified in LTE-based terrestrial broadcast of 5G standard Release 16 version, including RS pattern design for two numerologies, PBCH and PDCCH enhancement in CAS.

REFERENCES

[1] D. Gomez-Barquero, D. Navratil, S. Appleby, and M. Stagg, "Point-to-multipoint communication enablers for the fifth generation of wireless systems," *IEEE Commun. Stand. Mag.*, vol. 2, no. 1, pp. 53–59, Mar. 2018.

[2] ETSI. *Technical Specification Group Services and System Aspects; Multimedia Broadcast/Multicast Service (MBMS) User Services; Stage 1 (Release 6)*. Accessed: Jan. 2004. [Online]. Available: https://www.3gpp.org/ftp/Specs/archive/22_series/22.246/22246-600.zip

[3] ETSI. *Technical Specification Group Services and System Aspects; Multimedia Broadcast/Multicast Service; Stage 1 (Release 9)*. Accessed: Jun. 2008. [Online]. Available: https://www.3gpp.org/ftp/Specs/archive/22_series/22.146/22146-900.zip

[4] ETSI. *Technical Specification Group Services and System Aspects; Multimedia Broadcast/Multicast Service; Stage 1 (Release 10)*. Accessed: Dec. 2011. [Online]. Available: https://www.3gpp.org/ftp/Specs/archive/22_series/22.146/22146-a10.zip

[5] ETSI. *Technical Specification Group Services and System Aspects; Multimedia Broadcast/Multicast Service; Stage 1 (Release 11)*. Accessed: May 2013. [Online]. Available: https://www.3gpp.org/ftp/Specs/archive/22_series/22.146/22146-b10.zip

[6] ETSI. *Technical Specification Group Services and System Aspects; Multimedia Broadcast/Multicast Service; Stage 1 (Release 12)*. Accessed: Oct. 2014. [Online]. Available: https://www.3gpp.org/ftp/Specs/archive/22_series/22.146/22146-c00.zip

[7] M. Fuentes *et al.*, "Physical layer performance evaluation of LTE-advanced pro broadcast and ATSC 3.0 systems," *IEEE Trans. Broadcast.*, vol. 65, no. 3, pp. 477–488, Sep. 2019.

[8] D. Lecompte and F. Gabin, "Evolved multimedia broadcast/multicast service (eMBMS) in LTE-advanced: Overview and Rel-11 enhancements," *IEEE Commun. Mag.*, vol. 50, no. 11, pp. 68–74, Nov. 2012.

[9] A. Sengupta, "5G cellular broadcast—Physical layer evolution from 3GPP release 9 to release 16," *IEEE Trans. Broadcast.*, vol. 66, no. 2, Jun. 2020.

[10] ETSI. *Study on Scenarios and Requirements for Next Generation Access Technologies*. Accessed: Jul. 29, 2018. [Online]. Available: http://www.3gpp.org/ftp//Specs/archive/38_series/38.913/38913-f00.zip

[11] "Report of 3GPP TSG RAN meeting #81," ETSI MCC, San Diego, CA, USA, Jun. 2018. [Online]. Available: http://www.3gpp.org/ftp/TSG_RAN/TSG_RAN/TSGR_81/Docs/RP-181999.zip

[12] *New SID on LTE-Based 5G Terrestrial Broadcast*, Qualcomm Incorporat., San Diego, CA, USA, Jun. 2018. [Online]. Available: http://www.3gpp.org/ftp/TSG_RAN/TSG_RAN/TSGR_80/Docs/RP-181342.zip

[13] ETSI. *Study on LTE-Based 5G Terrestrial Broadcast*. Accessed: Mar. 27, 2019. [Online]. Available: https://www.3gpp.org/ftp/Specs/archive/36_series/36.776/36776-g00.zip

[14] J. J. Gimenez *et al.*, "5G new radio for terrestrial broadcast: A forward-looking approach for NR-MBMS," *IEEE Trans. Broadcast.*, vol. 65, no. 2, pp. 356–368, Jun. 2019.

[15] D. Gomez-Barquero, J. J. Gimenez, and R. Beutler, "3GPP enhancements for television services: LTE-based 5G terrestrial broadcast," in *Wiley Encyclopedia of Electrical and Electronics Engineering*, Wiley, 2020.

[16] Y. Xu, "Enhancements on coding and modulation schemes for LTE-based 5G terrestrial broadcast system," *IEEE Trans. Broadcast.*, vol. 66, no. 2, Jun. 2020.

[17] C. Cox, *An Introduction to LTE: LTE, LTE-Advanced, SAE, VoLTE and 4G Mobile Communications*. Chichester, U.K.: Wiley, 2014.

[18] ETSI. *Physical Channels and Modulation*. Accessed: Jun. 24, 2019. [Online]. Available: https://www.3gpp.org/ftp/Specs/archive/36_series/36.211/36211-f60.zip

[19] L. Zhang, Y. Wu, G. K. Walker, W. Li, K. Salehian, and A. Florea, "Improving LTE eMBMS with extended OFDM parameters and layered-division-multiplexing," *IEEE Trans. Broadcast.*, vol. 63, no. 1, pp. 32–47, Mar. 2017.

[20] ETSI. *Physical Layer Procedures*. Accessed: Sep. 28, 2019. [Online]. Available: https://www.3gpp.org/ftp/Specs/archive/36_series/36.213/36213-f70.zip

[21] *Analysis of CAS Reception*, Qualcomm Incorporat., Chongqing, China, Oct. 2019. [Online]. Available: http://www.3gpp.org/ftp/TSG_RAN/WG1_RL1/TSGR1_97/Docs/R1-1910733.zip

[22] *Potential Enhancement for CAS*, Huawei, HiSilicon, Prague, Czech Republic, Aug. 2019. [Online]. Available: http://www.3gpp.org/ftp/TSG_RAN/WG1_RL1/TSGR1_98/Docs/R1-1908712.zip

[23] *Analysis of CAS Reception*, Qualcomm Incorporat., Reno, NV, USA, May 2019. [Online]. Available: http://www.3gpp.org/ftp/TSG_RAN/WG1_RL1/TSGR1_97/Docs/R1-1907008.zip

[24] *Vienna Cellular Communications Simulators*, Inst. Telecommun., T. U. Wien, Vienna, Austria, Accessed: Apr. 13, 2018. [Online]. Available: www.tc.tuwien.ac.at/vccs/

[25] *Evaluation Results for LTE-Based 5G Terrestrial Broadcast*, EBU, BBC, IRT, Athens, Greece, Feb./Mar. 2019. [Online]. Available: http://www.3gpp.org/ftp/TSG_RAN/WG1_RL1/TSGR1_96/Docs/R1-1903284.zip

[26] *On New Numerologies for PMCH to Support Rooftop Reception*, Huawei, HiSilicon, Prague, Czech Republic, Aug. 2019. [Online]. Available: http://www.3gpp.org/ftp/TSG_RAN/WG1_RL1/TSGR1_98/Docs/R1-1908093.zip

[27] *Evaluation Results and Potential Enhancements*, Qualcomm Incorporat., Spokane, WA, USA, Nov. 2018. [Online]. Available: http://www.3gpp.org/ftp/TSG_RAN/WG1_RL1/TSGR1_95/Docs/R1-1813727.zip

[28] *On the New Numerology for PMCH to Support Mobility Based on Designed RS Patterns*, Shanghai Jiao Tong Univ., Prague, Czech Republic, Aug. 2019. [Online]. Available: http://www.3gpp.org/ftp/TSG_RAN/WG1_RL1/TSGR1_98/Docs/ R1-1908097.zip

[29] *Support of Longer Numerologies for Rooftop Reception*, Qualcomm Incorporat., Prague, Czech Republic, Aug. 2019. [Online]. Available: http://www.3gpp.org/ftp/TSG_RAN/WG1_RL1/TSGR1_98/Docs/R1-1908841.zip

[30] *New Numerology for PMCH to Support Rooftop Reception*, Shanghai Jiao Tong Univ., Prague, Czech Republic, Aug. 2019. [Online]. Available: http://www.3gpp.org/ftp/TSG_RAN/WG1_RL1/TSGR1_98/Docs/R1-1908096.zip

[31] *Support of Longer Numerologies for Rooftop Reception*, Qualcomm Incorporat., Chongqing, China, Oct. 2019. [Online]. Available: http://www.3gpp.org/ftp/TSG_RAN/WG1_RL1/TSGR1_98b/Docs/R1-1911360.zip

[32] *Analysis of CAS Reception*, Qualcomm Incorporat., Prague, Czech Republic, Aug. 2019. [Online]. Available: http://www.3gpp.org/ftp/TSG_RAN/WG1_RL1/TSGR1_98/Docs/R1-1908842.zip

[33] *Chairman's Notes of AI 6.2.4 LTE-Based 5G Terrestrial Broadcast*, Ad-Hoc Chair (Ericsson), Reno, NV, USA, Nov. 2019. [Online]. Available: http://www.3gpp.org/ftp/TSG_RAN/WG1_RL1/TSGR1_99/Docs/R1-1913377.zip

[34] ETSI. *Services Provided by the Physical Layer*. Accessed: Apr. 11, 2019. [Online]. Available: https://www.3gpp.org/ftp/Specs/archive/36_series/36.302/36302-f20.zip

Dazhi He received the Ph.D. degree in electronic engineering from Shanghai Jiao Tong University, Shanghai, China, in 2009, where he is currently an Associate Researcher with the Cooperative Medianet Innovation Center. His research interests include wireless communications, smart transmission, and heterogeneous network.

Wanting Wang received the B.Eng. degree from Wuhan University, Wuhan, China, in 2018. She is currently pursuing the master's degree in electronics and communications engineering with Shanghai Jiao Tong University. Her current research is mainly about the receiving methods and power optimization in a full-duplex cooperative NOMA network.

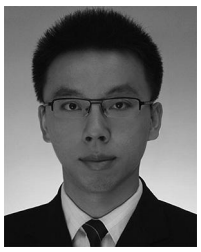

Yin Xu received the B.Sc. degree in information science and engineering from Southeast University, China, in 2009, and the master's and Ph.D. degrees in electronics engineering from Shanghai Jiao Tong University, 2011 and 2015, respectively, where he currently works as an Assistant Professor. He is active in participating in standardization progress in ATSC3.0 and 3GPP. He is interested in the theory and technology on converged broadcasting and broadband networks. His main research interests include channel coding, advanced bit-interleaved coded modulation and other physical layer technologies in broadcasting and 5G.

Xiuxuan Huang received the B.Eng. degree from the Nanjing University of Science and Technology, Nanjing, China, in 2018. She is currently pursuing the master's degree in electronics and communication engineering with Shanghai Jiao Tong University. Her current research interests include innovative techniques in frame structure and interleaving in broadband/broadcast system.

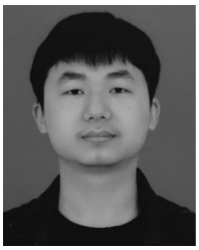

Hao Cheng received the B.Eng. degree in communication engineering from the University of Electronic Science and Technology of China in 2018. He is currently pursuing the master's degree in electronic engineering with the Cooperative Media Network Innovation Center, Shanghai Jiao Tong University. His current research interests include system-level simulation for broadcast networks.

Xiaohan Duan received the B.Eng. degree from the Dalian University of Technology. She is currently pursuing the master's degree in information and communication engineering with Shanghai Jiao Tong University. Her research field is nonuniform constellations in communication system.

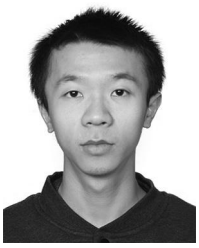

Yihang Huang received the bachelor's degree from the University of Electronic Science and Technology of China in 2014. He is currently pursuing the Ph.D. degree in information and communication engineering with Shanghai Jiao Tong University. His research interests include digital signal processing and cooperative transmission by DTTB and cellular networks.

Hanjiang Hong received the B.Eng. and M.Eng. degrees from Shanghai Jiao Tong University, Shanghai, China, in 2016 and 2019, respectively. She is currently pursuing the Ph.D. degree in information and communication engineering with Shanghai Jiao Tong University. Her current research interests include innovative techniques in bit-interleaved coding and modulations, such as nonuniform constellations and converged broadband/broadcast systems.

Yiwei Zhang received the B.S. degree in engineering from Northwestern Polytechnical University, Xi'an, China, in 2016. He is currently pursuing the Ph.D. degree with the Cooperative Media Network Innovation Center, Department of Electronic Information and Electrical Engineering, Shanghai Jiao Tong University. His research interests include wireless communications, broadcast and multicast optimization, and heterogeneous networks.

Wenjun Zhang (Fellow, IEEE) received the B.S., M.S., and Ph.D. degrees in electronic engineering from Shanghai Jiao Tong University, Shanghai, China, in 1984, 1987, and 1989, respectively. After three years as an Engineer with Philips, Nuremberg, Germany, he returned to Shanghai Jiao Tong University and became a Full Professor of electronic engineering in 1995. He was one of the main contributors of the Chinese DTTB Standard issued in 2006. He holds 142 patents and has published 110 papers in international journals and conferences. He is the Chief Scientist of the Chinese Digital TV Engineering Research Centre (NERC-DTV), an industry/government consortium in DTV technology research and standardization, and the Director of the Cooperative MediaNet Innovation Center, an excellence research cluster affirmed by the Chinese Government. His main research interests include video coding and wireless transmission, multimedia semantic analysis, and broadcast/broadband network convergence.